Am J Transl Res 2018;10(11):3370-3384
www.ajtr.org /ISSN:1943-8141/AJTR0078798

Original Article

G-protein-coupled receptor kinase-5 promotes glioblastoma progression by targeting the nuclear factor kappa B pathway

Yang Yang[1,2,3], Jing-Jing Wu[4,5], Chuan-Dong Cheng[1,2,3], De-Jun Bao[1,2,3], Yong-Fei Dong[1,2,3], Dong-Xue Li[1,2,3], Wan-Xiang Niu[1,2,3], Chen-Xu Zhou[1,2,3], Chao-Shi Niu[1,2,3]

[1]Shandong University, Jinan, Shandong Province, P. R. China; [2]Department of Neurosurgery, The First Affiliated Hospital of University of Science and Technology of China, Hefei 230001, Anhui Province, P. R. China; [3]Anhui Province Key Laboratory of Brain Function and Brain Disease, Hefei 230001, Anhui Province, P. R. China; [4]Institute of Clinical Pharmacology of Anhui Medical University, Key Laboratory of Anti-Inflammatory and Immune Medicine, Ministry of Education, Anhui Collaborative Innovation Center of Anti-Inflammatory and Immune Medicine, Hefei 230032, Anhui Province, P. R. China; [5]Department of Oncology, The Second Affiliated Hospital of Anhui Medical University, Hefei 230601, Anhui Province, P. R. China

Received May 1, 2018; Accepted October 21, 2018; Epub November 15, 2018; Published November 30, 2018

Abstract: G-protein-coupled receptor kinase-5 (GRK5) plays essential roles in multiple celluar events. However, its role in the development and progression of glioma is poorly understood. In this research, we found that GRK5 is significantly upregulated in human gliomas. For the first time, a close relationship was noted between GRK5 expression and blood vessel development in human glioma. Specifically co-expression of GRK5 and the tumor stem cell marker CD133 was observed in the cytoplasm of high grade glioma cells. The depletion of GRK5 suppressed the proliferation, migration and invasion in glioma cells, and promoted apoptosis. We next discovered that GRK5 knockdown inhibits the nuclear factor kappa B (NF-κB) pathway, thus resulting in downregulation of key downstream secretory products CCL2, IL-6 and IL-8 in glioma cell conditioned medium (CM). In addition, treatment of cells with the NF-κB stimulator PMA reversed this effect and increased the GRK5 level. Our results demonstrate an oncogenic role for GRK5 and reveal an activation of the GRK5-NF-κB pathway during the malignant progression of glioma.

Keywords: Glioma, G-protein-coupled receptor kinase-5, nuclear factor kappa B, proliferation, glioma stem cell, blood vessel

Introduction

About 80% of intracranial primary malignant tumor are gliomas. Glioblastoma multiforme (GBM) is one of the most lethal types of human cancer [1, 2]. Despite numerous advances in chemotherapeutic protocols, GBM therapy still relies on the palliative efficacy of a combination of surgery, radiation and temozolomide [1, 2]. Due to GBM's extremely malignant characteristics, such as robust invasiveness, rapid proliferation and increased angiogenesis, patients with GBM have a median survival time of only 14 months [1, 2].

G protein-coupled receptor kinases (GRKs) belong to the serine/threonine kinase family that bind and phosphorylate agonist-activated G protein-coupled receptors (GPCRs), leading to their desensitization [3]. Seven GRK subtypes (GRK1-7) have been characterized and divided into three groups according to their sequence homology [3-5]. Studies demonstrate that GRK expression and activity are impaired in many pathological conditions [6-8]. Among the GRKs, GRK5 is the most studied due to its involvement in several pathologic conditions, including cancer [9, 10]. Indeed, GRK5 inhibit cancer progression through the desensitization of GPCR or non GPCR-receptors [11-18], as well as stimulate tumor growth by acting on non-receptor substrates [19-27]. Chromosome translocation in the region of 10q24 has been observed in several tumors, including glioma [28-30], suggesting that an alteration of genes in this region can affect tumor progression. Since GRK5

maps on chromosome 10 at the region of q24, it is likely that there is a correlation between an alteration in GRK5 expression and certain glial tumors [31].

The NF-κB family of widely expressed transcription factors, regulate cell cycle progression, cell proliferation and apoptosis in tumors [32-35]. A previous study reported that NF-κB regulates GBM secretion. Inhibition of the NF-κB pathway resulted in the downregulation of IL8, IL6, CCL2, IL-1β and CXCL14 and in the inhibition of their related pathways [33]. GRK5 is an important regulator of NF-κB signaling, and it can enhance its activity. Conversely, p50 and p65 can also directly bind to GRK5 DNA in the nucleus, thus upregulating the GRK5 level [36-40]. However, the role of GRK5 in the GBM is so far poorly understood, which prompted us to examine the correlation between GRK5 expression and NF-κB signaling in gliomas.

The aim of this study was to detect GRK5 expression in human gliomas and to explore the relationship between GRK expression and biological activity in gliomas. By qRT-PCR, western blotting and immunohistochemistry, we confirmed in a cohort of 110 specimens that GRK5 was widely distributed throughout gliomas and frequently located near blood vessels. We also found co-expression between GRK5 and CD133 using double-immunofluorescence. A GRK5-knockdown stable cell line (GRK5-KD) was generated by using the lentivirus transfection method. Migration and invasion were weakened in GRK5-knockdown cells by performing a wound healing assay and a transwell assay, respectively. A xenograft model was established and a CCK-8 assay was performed to detect decreased cell proliferation in gliomas in vitro and vivo. The number of apoptotic cells increased by flow cytometry. Furthermore, we use a known NF-κB stimulator, phorbol myristate acetate (PMA), to investigate the interaction between GRK5 and NF-κB signaling in glioma cells by western blotting. Lastly, ELISA quantification showed that GRK5 knockdown decreased the levels of CCL2, IL-6 and IL-8 in the CM of glioma cells.

Methods

Clinical samples

According to histopathological features, such as mitotic activity, atypia, anaplasia, microangiogenesis and necrosis, the World Health Organization (WHO) has traditionally divided gliomas into four grades [41]. Generally, grades I and II are low grade gliomas (LGG), whereas grades III and IV are high grade gliomas (HGG). Furthermore, grade I tumors lack these histopathological features, whereas grade II tumors are atypical [42].

All patients were diagnosed with glioma at the Department of Neurosurgery, the First Affiliated Hospital of University of Science and Technology of China. None of the patients had received chemotherapy or radiotherapy before surgery. From 2010 to 2016, glioma specimens (n = 110) were obtained from these patients during the initial surgery. For the control, normal adult brain specimens (n = 10) were obtained from patients with severe traumatic brain injury needing decompression surgery. After surgical resection, portions of the tumor specimens were sent for routine neuropathological evaluation, whereas the remaining specimens were immediately frozen in liquid nitrogen. After evaluation by three neuropathologists and classification according to WHO 2007 classification criteria. The specimens (n = 110) were classified as 30 low-grade gliomas (LGG, WHO grade II) and 80 high-grade gliomas (HGG, WHO grades III 36 and IV 44). Informed consent was obtained from all patients before surgery. All research methods and procedures were approved by the Ethics Committee of the First Affiliated Hospital of University of Science and Technology of China.

Cell culture, and lentivirus production and cell infection

The glioblastoma cell lines U251, U87 and T98G were purchased from the Chinese Academy of Sciences Type Culture Collection (Shanghai, China). Cells were maintained in Dulbecco's modified Eagle's medium (DMEM; Gibco, USA) supplemented with 10% fetal bovine serum (FBS) (Hyclone, USA) in a humidified incubator at 37°C with 5% CO_2 [43, 44].

GRK5-knockdown lentiviral solution was obtained from GenePharma (Shanghai, China). Lentiviruses were packaged in HEK293T cells, and according to the manufacturer's instructions, they were used to infect U251 cells in the presence of 1 μg/ml polybrene (Sigma, USA). In medium supplemented with 5 μg/ml puromycin (Sigma, USA), infected cells were subcultured

to 10% confluence. Untreated U251 cells with defined as the blank group (i.e., control), whereas cells expressing LV3-GRK5-knockdown-GFP or LV3-negative control-GFP were defined as the GRK5-KD or NC group, respectively. GRK5 expression was detected by quantitative reverse transcriptase-polymerase chain reaction (qRT-PCR) and western blotting [43, 44].

RNA isolation and qRT-PCR

Using the Qiagen RNeasy Mini Kit, total RNA was extracted from normal brain specimens, glioma specimens and glioblastoma cells. Thereafter, 2 mg of RNA was reverse transcribed to cDNA using the RevertAid First Strand cDNA Synthesis Kit. All procedures were performed according to the manufacturer's instructions. The GRK5 expression level was detected by qPCR using the AceQ SYBR Green Master Mix (Vazyme, China). The fold change in gene expression was calculated using the $2^{-\Delta\Delta Ct}$ method [44, 45]. The primer sequences were as follows: GRK5, forward: 5'-GGCTGCAGAGGTCAAGAGAC-3', reverse: 5'-TGTCCAGCACGTCCTTACAG-3'; and β-actin, forward: 5'-ATGGATGATGATATCGCCGCGCTC-3'; reverse: 5'-TTTCTCCATGTCGTCCCAGTTGG-3'.

Western blotting

Western blotting was performed as previously described [44, 48]. Monospecific antibodies against human GRK5 (Sigma, USA, 1:400), p65 (Sigma, USA, 1:500), p50 (Sigma, USA, 1:500), pIκ-Bα (Sigma, USA, 1:400) and Bcl-2 (Beyotime, China, 1:500) were used at 4°C overnight. A monospecific antibody against β-actin (1:1000) was used at room temperature for 1 h, immunoreactive proteins were visualized by chemiluminescence using an ECL Detection System (BeyoECL Plus, Beyotime). Protein band intensity were determined using Image Pro Plus 6.0 Software (Japan). To investigate crosstalk between GRK5 and NF-κB pathway, U251 cells were maintained in the presence or absence of phorbol myristate acetate (PMA, 20 nM, Sigma, USA) for 24 h [36].

Cell migration assay

Cells from GRK5-knockdown (GRK5-KD) and negative control (NC) groups were cultured in 12-well plates. The monolayer of cells was lifted from 12-well plates with a standard 200 μl micropipette tip when cells reached 80-90% confluence. At 24, 48 and 72 h, we observed cell migration into the scraped area, images were captured at fixed observation points [44] using a IX71 model microscope (Olympus, Japan). Cell migration was determined by measuring the movement of cells into the scraped area. Quantitative analysis was performed with Image J software, and results were expressed as a percentage: the mean of the wound closure area relative to the mean of the initial wound area. This experiment was repeated three times.

Matrigel invasion assay

The invasion assay was performed using BioCoat™ Invasion Chambers (BD, USA). After coating the upper chamber with Matrigel, approximately 5×10^4 cells were resuspended in 200 μl of serum-free DMEM and added into the upper chamber, while 600 μl of DMEM supplemented with 10% FBS was added into the lower chamber. After culturing for 18 h at 37°C, when cells on the upper side of the membrane were removed, the invaded cells on the lower membrane surface were fixed in 1% paraformaldehyde, stained with 0.1% crystal violet. After that, the invaded cells were counted under a light microscope in 8 random 200× fields per insert. Cell counts were expressed as the average cells number per field of view [46]. This experiment was repeated three times.

Cell proliferation assay

Cell proliferation was measured using the Cell Counting Kit-8 (CCK-8, DOJINDO, Japan). In brief, an equal number of glioma cells was seeded into a 96-well plate. After culturing for 48 h, the media was replaced with that containing a 1:10 dilution of CCK-8. After incubating for an additional 2 h at 37°C, the absorbance was measured using a spectrophotometer set at 450 nm. This experiment was repeated three times.

In vivo xenograft model

A human xenograft model was established as previously described [44]. After subcutaneously injecting approximately 5×10^6 stably transfected glioblastoma cells, a tumor xenograft model was established in female BALB/c athymic mice (Cancer Institute of The Chinese

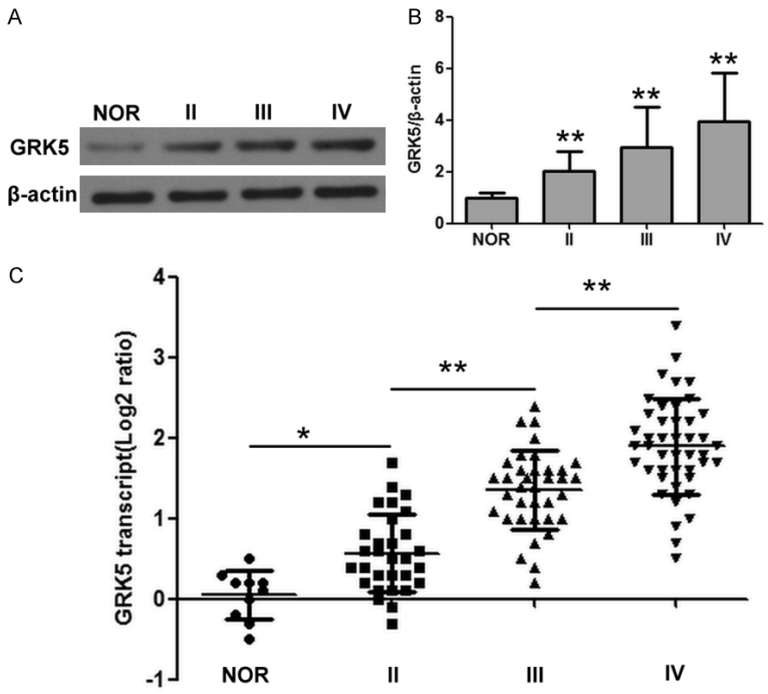

Figure 1. GRK5 expression in glioma specimens of different pathological grades. A. GRK5 expression by western blotting in normal brain (control) and grade II, III and IV glioma specimens. B. Histogram summarizting the relative GRK5 protein level as determined by western blotting analysis (**, $P < 0.01$, compared to NOR). C. By qRT-PCR, GRK5 expression in low grade gliomas was lower than in high grade gliomas (*, $P < 0.05$, **, $P < 0.01$, compared to NOR). NOR, normal brain tissue; II, WHO II gliomas; III, WHO III gliomas and IV, WHO IV gliomas.

Academy of Medical Science). U251 cells served as the blank group (control; a total of 18 mice, with n = 6 per group). All experimental procedures were performed in according to the approved Shandong University guidelines approved by Institutional Animal Care. The xenograft tumor volume was continuously measured twice a week, and tumor growth was calculated as follows: volume = length × width^2/2. Nude mice were sacrificed after 33 days, and tumors were harvested and weighed.

Immunohistochemistry

Immunohistochemical experiments were performed as previously described. Paraffin cross-sections of human glioma specimens were used to detect GRK5, Ki67 and CD34 and to correlate their distribution with proliferation and angiogenesis [44, 47-49]. Mouse anti-GRK5 (1:400; Sigma, USA), mouse anti-Ki67 (1:400; Sigma, USA) and rabbit anti-CD34 (1:400; Abcam, UK) were used as the primary antibodies. For the negative control, the primary antibody was replaced with phosphate-buffered saline (PBS). After incubating with a biotinylated secondary antibody, the color reaction were carried out with diaminobenzidine. Thereafter, cross-sections were lightly counterstained with Mayer's haematoxylin and mounted.

According to the percentage of immunopositive cells, we scored each cross section as follows: 0, < 5% of cells were positive; 1(+), 5% to < 25% of cells were positive; 2(++), 25% to 75% of cells were positive and 3(+++), > 75% of cells were positive. We then graded the intensity of positive staining as follows: 0, negative; 1(+), weak; 2(++), strong. By adding the immunopositivity and intensity scores as previously described [47-49], the combined total scores were obtained (range, 0-5(+++++)). Cases with a total score of 0 to 2(++) were assigned to the low expression group; whereas cases with a total scores of 3(+++) to 5(+++++) were assigned to the high expression group. All specimens were scored by three independent pathologists without knowledge of the relevant clinical data [47-49].

Immunofluorescence staining

Double-labeling immunofluorescence combined with confocal laser scanning microscopy (CLSM) was carried out to detect the expression of GRK5 and the tumor stem cell maker CD133 in glioma specimens. After fixing with formaldehyde, deparaffinizing with xylene and rehydrating in PBS, the paraffin cross-sections were incubated in 3% hydrogen peroxide to quench endogenous peroxidase activity for 25 min. After blocking with 10% normal goat serum for 1 h, the cross-sections were incubated with anti-GRK5 (IgG, 1:400; Sigma) and anti-CD133 (IgG, 1:400; Abcam) antibodies at 4°C overnight, followed by FITC- and TRITC-conjugated secondary antibodies for 1 h at room tempera-

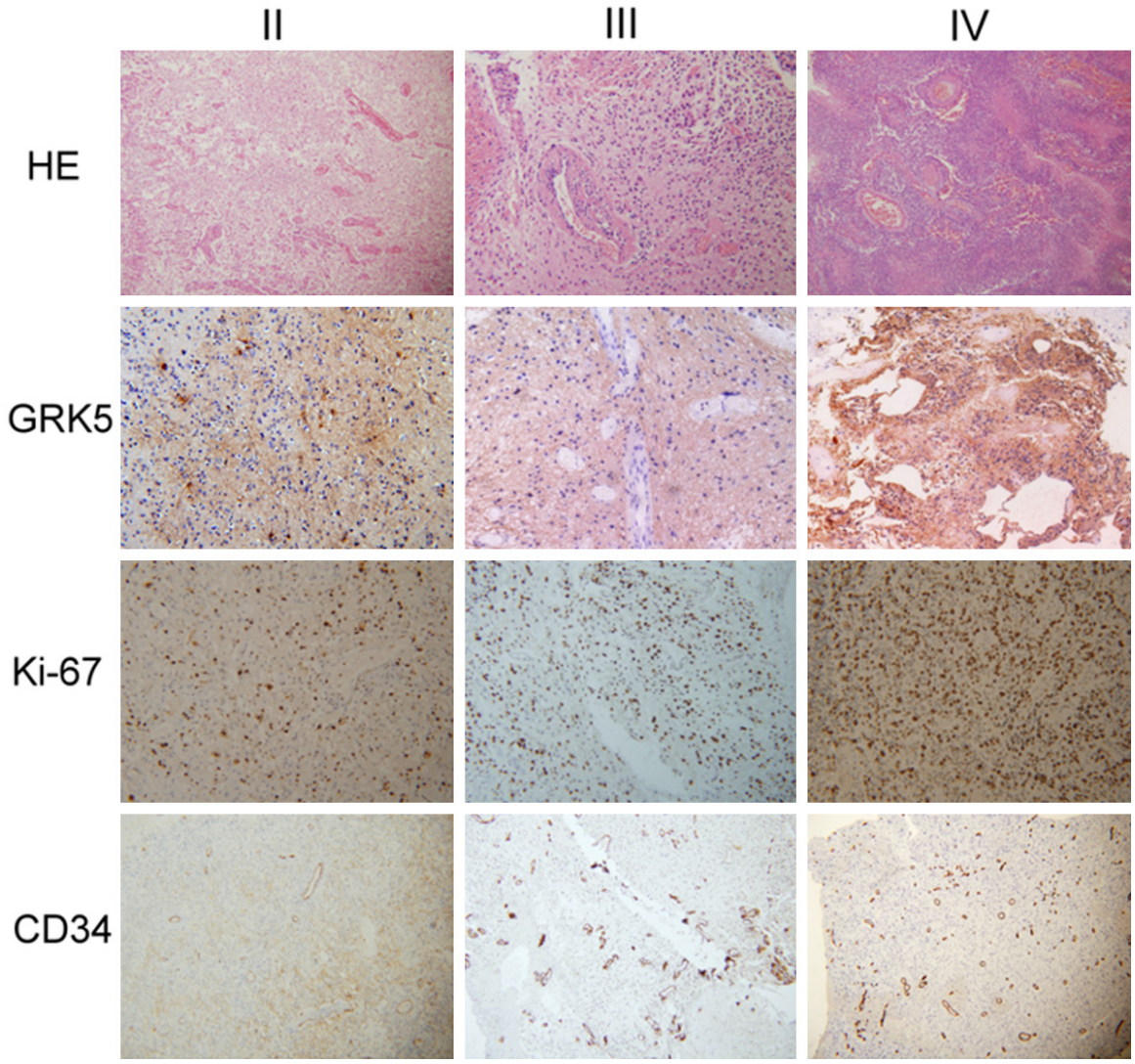

Figure 2. Immunohistochemical analysis of the expression patterns of GRK5, Ki67 and CD34 in glioma specimens of different pathological grades (magnification, ×100). GRK5 was highly expressed in human gliomas, and its expression was positively correlated with the pathological grade ($P < 0.01$, Spearman's rank-sum test). There was a positive correlation between GRK5 and Ki-67 expression in human gliomas ($P < 0.05$, Spearman's rank-sum test), as well as between GRK5 and CD34 expression ($P < 0.05$, Spearman's rank-sum test).

Table 1. Correlation between GRK5 and Ki-67 expression in gliomas

	Low GRK5	High GRK5	P
Low Ki-67	11	16	0.013
High Ki-67	32	51	

ture [47-49]. All images were obtained using an Olympus CLSM.

Enzyme-linked immunosorbent assay (ELISA)

For the ELISA (Cloud-Clone Corp, USA), approximately 5 × 10^3 glioblastoma cells were seeded into each well of a 96-well plate. Cells were maintained in DMEM in the presence or absence of 20 nM PMA for 24 h before the assay. Thereafter, 50 µl of cell conditioned medium (CM), CCL2, IL-8 and IL-6 secreted by glioblastoma cells, was analyzed after 24 h of culture [33]. This experiment was repeated three times.

Apoptosis assay

For the apoptosis assay, tumor cells were simultaneously stained with Annexin V-PE and the viability dye 7-amino-actinomycin D (7AAD)

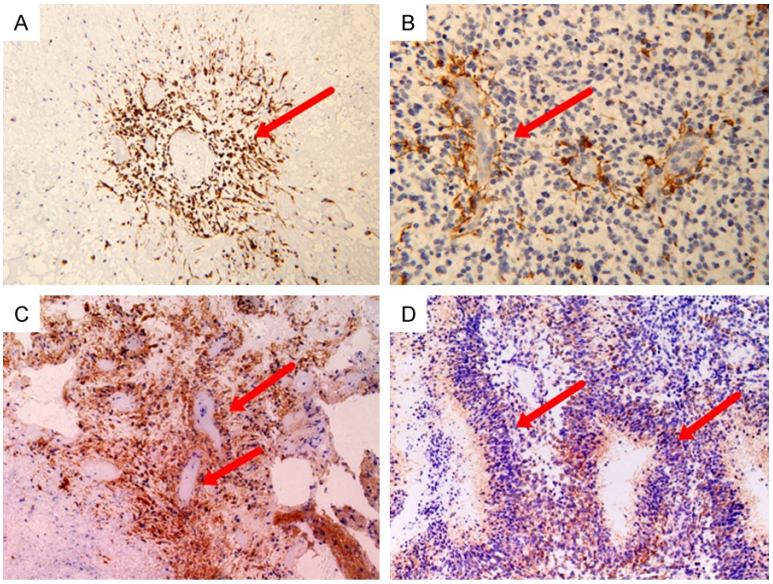

Figure 3. GRK5 localized predominantly in human gliomas (magnification, ×200). GRK5 predominantly located near blood vessels in human gliomas (red arrow), specifically close to the lumen of several blood vessels. (A) Case 1 had WHO II glioma, (B) Case 2 had WHO III glioma, (C) Case 3 and (D) Case 4 both had WHO gliomas.

Table 2. Correlation between GRK5 and CD34 expression in gliomas

	Low GRK5	High GRK5	P
Low CD34	13	10	0.020
High CD34	30	57	

using the Annexin V-PE/7-AAD Apoptosis Detection Kit (KeyGen Biotech, China) according to the manufacturer's instructions. Stained cells were immediately analyzed by flow cytometry (Cell Lab Quanta SC; Beckman Coulter, USA) [44]. This experiment was repeated three times.

Statistical analysis

All experiments, except for the xenograft tumor assay and immunohistochemistry experiments, were conducted at least three times. All statistical analyses were performed using SPSS 22.0 Software. The independent Student's *t*-test was used to compare the expression level of a target gene between two groups. One-way analysis of variance (ANOVA) was used to compare the expression level of a target gene between three groups. Spearman's rank-sum test was used to correlate the expression level of a target gene in different grade gliomas. *P*-values less than 0.05 were considered statistically significant.

Results

GRK5 expression in human gliomas was positively correlated with pathological grade

To explore the relationship between GRK5 expression and pathology grade in gliomas, we analyzed mRNA and protein levels by qRT-PCR (10 normal brain tissues and 110 glioma samples) and western blot (total 33 samples: 8 normal brain tissues, 8 WHO II samples, 8 WHO III samples and 9 WHO IV samples), respectively. Firstly, qRT-PCR data showed that GRK5 is upregulated in glioma specimens of different pathological grade, compared to normal human brain specimens (**Figure 1C**, $P < 0.05$, independent Student's *t*-test). Further research also showed that the relative GRK5 mRNA level was significantly higher in HGGs than that in the LGGs (GRK5 mRNA level: $F = 59.784$, $P < 0.01$, ANOVA). Secondly, western blotting also showed that the GRK5 protein level was upregulated in gliomas (**Figures 1A**, **1B**, S1 and S2; independent Student's *t*-test). There was an association between higher GRK5 expression and high malignancy in glioma specimens (GRK5 protein level: $F = 38.351$, $P < 0.01$, ANOVA) (**Figure 1A**, **1B**).

Furthermore, immunohistochemical analysis (30 WHO II samples, 36 WHO III samples and 44 WHO IV samples) also showed that GRK5 was mainly confined in the cytoplasm, and its degree of enrichment in the cytoplasm of LGGs was low, whereas in the cytoplasm of HGGs, the degree of enrichment was high. Our data indicated that GRK5 expression was positively correlated with pathological grade ($r = 0.250$, $P = 0.008 < 0.01$, the Spearman's rank-sum test) (**Figure 2**). We also found a positive correlation between GRK5 and Ki-67 by immunohistochemical analysis ($r = 0.236$, $P = 0.013 < 0.05$, the Spearman's rank-sum test) (**Figure 2** and **Table 1**).

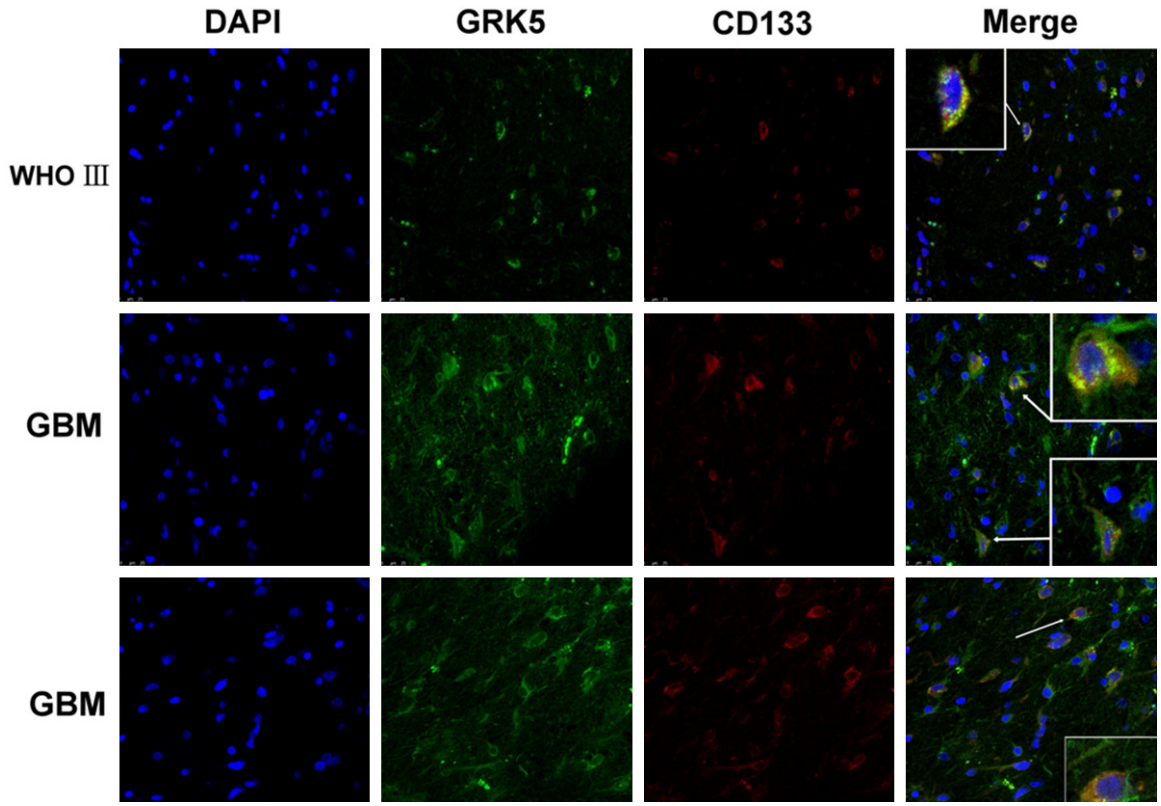

Figure 4. GRK5 and CD133 co-localization in glioma specimens using double-immunofluorescence. GRK5/CD133 co-expression were observed in WHO III gliomas and GBMs. DAPI (4,6-diamidino-2-phenylindole) indicated nuclear (blue). GRK5 (green) mainly expressed in the cytoplasm of glioma cells, while tumor stem cell-related marker CD133 was located in the cytoplasm of a part of high grade glioma cells. The co-localization was shown in yellow (merge, magnification, arrows). Scale bar, 25 μm.

GRK5 is a closely associated with tumor blood vessels and is co-expressed with the tumor stem cell marker CD133 in gliomas

By immunohistochemistry, we found a positive correlation between GRK5 and the vessel marker CD34 (r = 0.222, P = 0.020 < 0.05, the Spearman's rank-sum test) (**Figures 2**, **3** and **Table 2**). Furthermore, GRK5 expression was detected close to the lumen of several tumor blood vessels in human gliomas (**Figure 3**). By dual immunofluorescence analysis (8 WHO III samples and 15 WHO IV samples), GRK5/CD133 co-expressing cells were detected in several High grade glioma specimens. It was found that most CD133+ cells co-expressed GRK5 in HGGs (**Figure 4**).

Down-regulation of GRK5 inhibits migration and invasion in U251 cells

Firstly, the relative expression of GRK5 in different cell lines (U87, U251 and T98G) was detected. We found that the GRK5 mRNA level was relatively higher in U251 cells than that in the other glioma cell lines (P < 0.05, ANOVA) (**Figures 5A-C**, S3). Using lentivirus transfection, a GRK5-knockdown stable cell line was generated (**Figure 5G**). Green fluorescent signal was detected in > 98% transfected cells. GRK5 expression was detected by qRT-PCR and western blotting. It was found that the GRK5 level was significantly decreased in GRK5-KD cells, whereas in the NC group, GRK5 expression did not markedly change compared to U251 cells (P < 0.01, ANOVA) (**Figures 5D-F**, S4). We next detected whether GRK5 expression was related to the invasion of glioblastoma cells. The transwell assay showed that the down-regulation of GRK5 significantly inhibited cell invasion (P < 0.01, ANOVA) (**Figure 6A**, **6B**). On the other hand, the wound healing assay showed that GRK5 knockdown slowed the wound closure speed of tumor cells (P < 0.01, ANOVA) (**Figure 6C**, **6D**). These studies indicated that

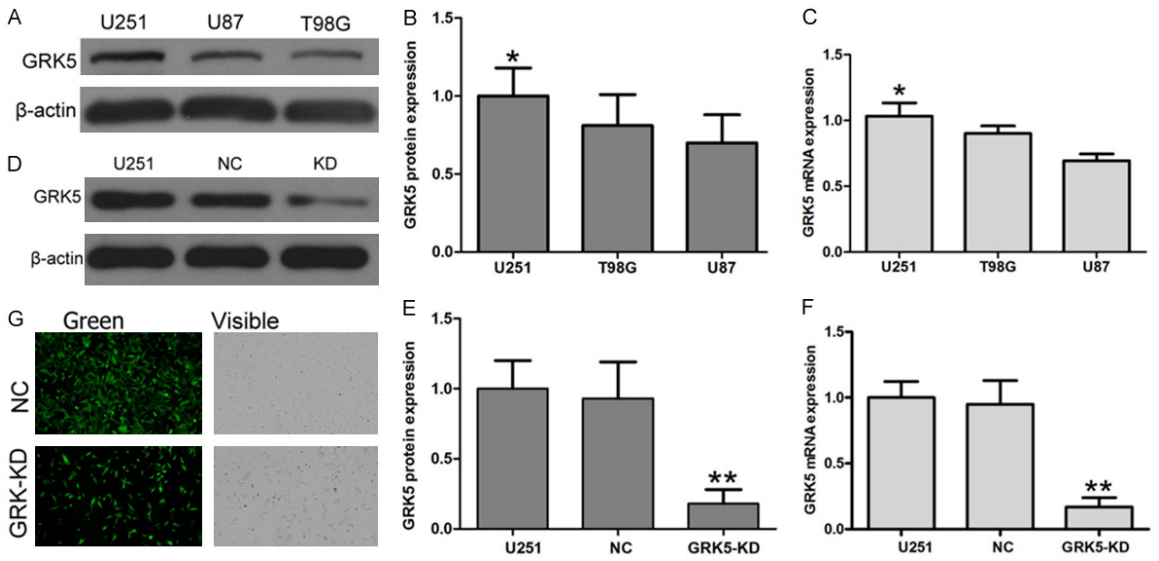

Figure 5. GRK5-knockdown stable cell line was generated with lentivirus transfection method. A. Detection of GRK5 relative expression levels in U251, U87 and T98G cells by Western blot. B. Histogram summarizing the relative GRK5 level in U251, U87 and T98G cells as determined by western blot analysis. (*, $P < 0.05$, compared to U87 cells and T98G cells). C. Histogram summarizing the relative GRK5 level in U251, U87 and T98G cells as determined by qRT-PCR (*, $P < 0.05$, compared to U87 cells and T98G cells). D. Detection of GRK5 protein expression in U251 cells by Western blot. E. Histogram summarizing the relative GRK5 level in U251 cells as determined by western blot analysis (**, $P < 0.01$, compared to the NC group). F. Histogram summarizing the relative level of GRK5 mRNA in U251 cells by qRT-PCR (**, $P < 0.01$, compared to the NC group). G. Establishment of GRK-knockdown stable cell lines (magnification, ×200). Data were mean ± SD from three independent experiments.

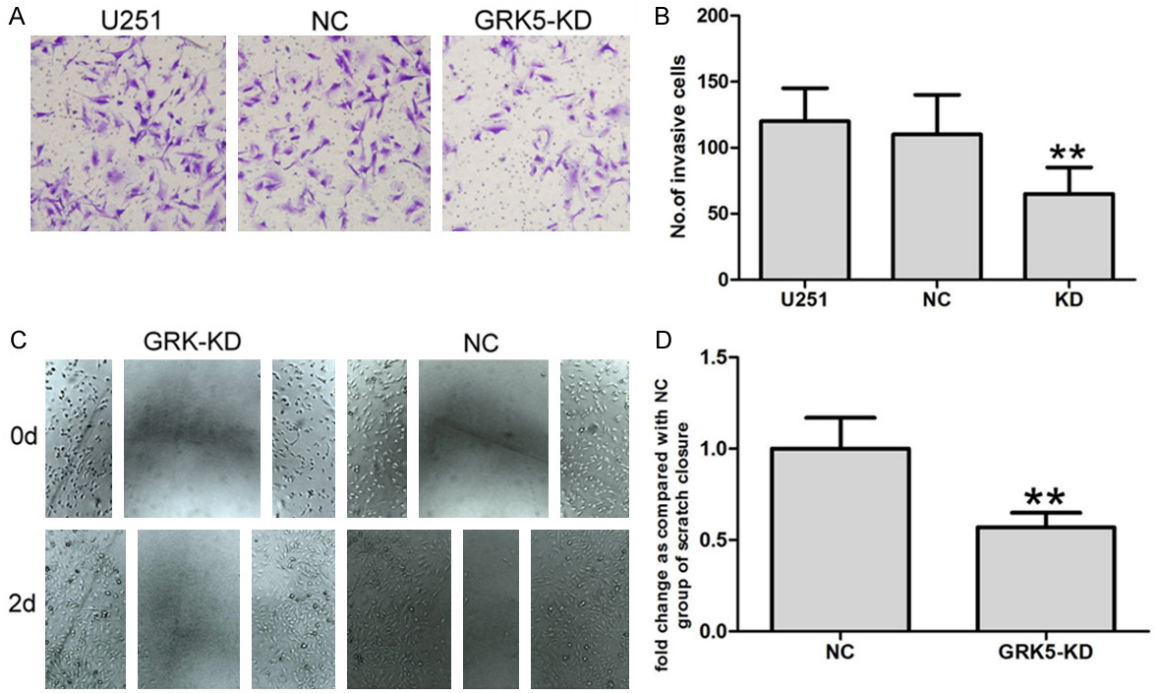

Figure 6. GRK5 knockdown inhibits the migration and invasion of glioblastoma cells. A. The number of invasive cells was determined using the transwell matrix penetration assay (with Matrigel) (magnification, ×200). B. Histogram summarizing the number of invasive cells per 200× field (*, $P < 0.05$, compared to the NC group). C. GRK5 knockdown inhibited the wound closure speed of U251 cells (magnification, ×200). D. Histogram summarizing the fold change in wound closure as compared with the NC group (**, $P < 0.01$, compared to the NC group). Data were mean ± SD from three independent experiments.

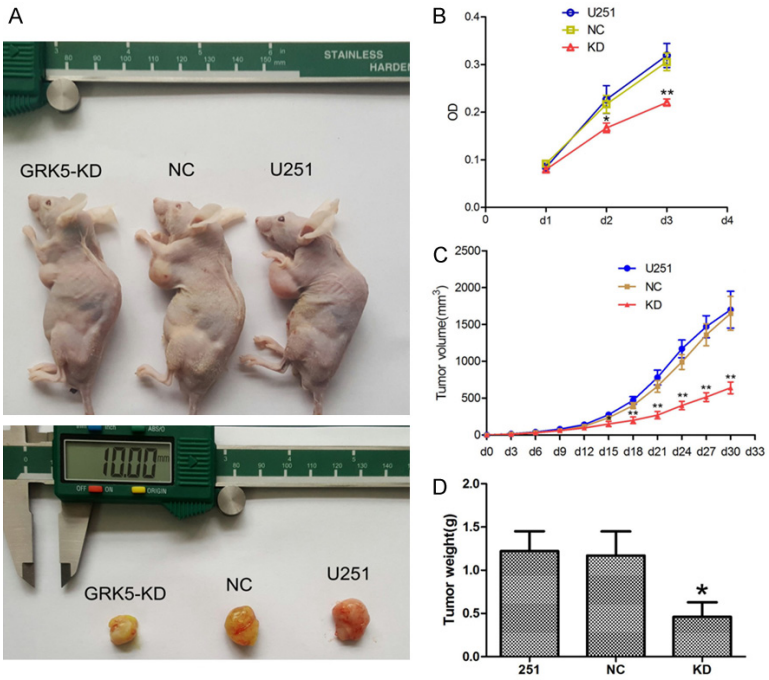

Figure 7. GRK5 knockdown reduced the proliferation of U251 glioblastoma cells in vitro and vivo. A. The establishment of the xenograft tumor model. GRK5-KD tumor xenografts were visibly smaller than those of the NC and U251 groups. B. Measurement of glioblastoma cell proliferation using the CCK-8 assay. A significant difference in glioblastoma cell growth was observed after GRK5 knockdown in glioblastoma cells (*, $P < 0.05$, **, $P < 0.01$, compared to the NC group). C. Tumor growth curves for glioblastoma tumor xenografts (*, $P < 0.05$, **, $P < 0.01$, compared to the NC group). D. Histograms summarizing tumor mass for glioblastoma tumor xenografts (n = 6 for each group; *, $P < 0.05$, compared to the NC group). Data were mean ± SD from three independent experiments.

GRK5 can significantly promote the invasion and migration of glioblastoma cells.

Down-regulation of GRK5 inhibits the proliferation of U251 cells in vitro and vivo

The effect of GRK5 on glioblastoma cell proliferation was examined by the CCK-8 assay. The viability of GRK5-KD cells significantly decreased compared to NC cells (**Figure 7B**).

The role of GRK5 in vivo was confirmed by the tumor xenograft model (**Figures 7A**, **7C**, **7D**, S7). After 30 days of subcutaneous inoculation, the cell suspension inoculation developed into a solid tumor xenograft in each mouse (**Figures 7A**, S7). The growth curve of tumor xenografts showed that the down-regulation of GRK5 slowed tumor growth in vivo, and no statistical difference was observed between NC and U251 groups (**Figure 7C**). Mice were euthanized on day 33. The average tumor weight in mice of the NC group was higher than that in mice of the GRK5-KD group (**Figure 7D**). These findings suggested that GRK5 may promote the growth of gliomas in vitro and vivo.

Down-regulation of GRK5 promotes the apoptosis of U251 cells

As mentioned above, GRK5 is an important regulator of NF-κB signaling that regulates cell proliferation, cell cycle progression and apoptosis [37-40]. To further confirm the role of GRK5 in glioblastoma cells, the number of apoptotic cells was determined by flow cytometry (**Figure 8A**, **8B**). Using Annexin V-PE/7-amino-actinomycin D double-stained U251 cells, the externalization of phosphatidylserine was detected by flow cytometry. The percentage of apoptotic cells significantly increased in GRK5-KD cells (42.35 ± 3.56)% compared with those of the NC (4.45 ± 0.51)% and U251 group (2.68 ± 0.31)% ($P < 0.01$, ANOVA). The Bcl-2 family is an important regulatory factor in various apoptotic pathways. The loss of GRK5 down-regulated the Bcl-2 protein level (**Figures 8C**, **8D**, S5) ($P < 0.01$, ANOVA). These data suggested that GRK5 may have the ability to induce apoptosis in glioblastoma cells.

Activation of the GRK5-NF-κB signaling pathway is involved in the progression of glioma

Previous research reported that PMA can regulate NF-κB activation and increase the expression of GRK5 [50, 51]. Using the known NF-κB stimulator PMA, the relationship between GRK5 and the NF-κB pathway in gliomas was investigated by western blot analysis (**Figures 9A**, **9B**, S6). After 24 h of PMA treatment, the expression of phosphorylated Iκ-Bα (pIκ-Bα), p50, p65 and GRK5 was increased, suggesting that PMA can increase the levels of GRK5-NF-κB signaling proteins in glioblastoma cells

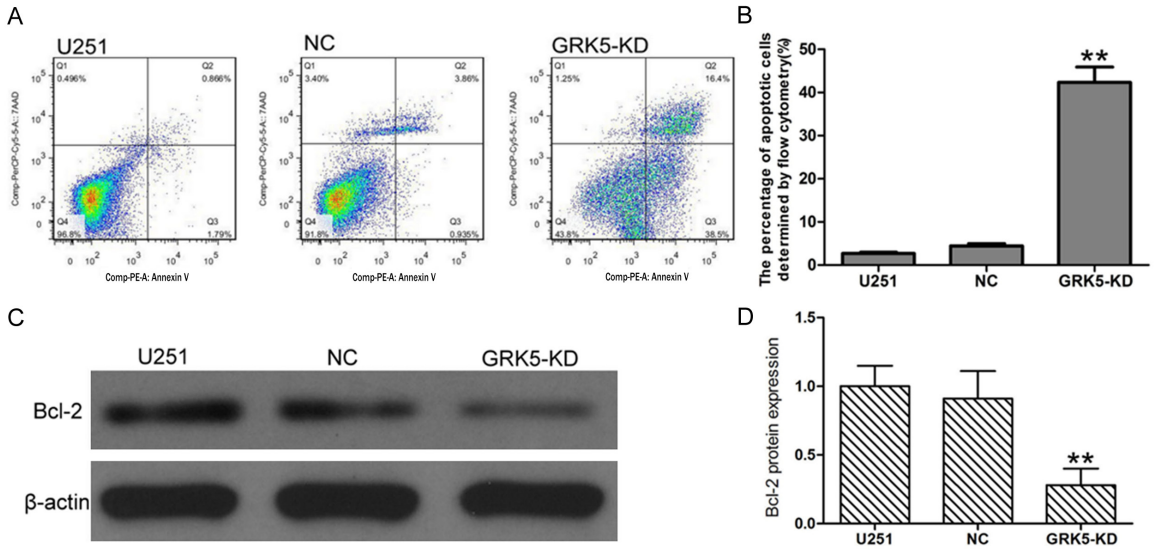

Figure 8. GRK5-knockdown promotes glioma apoptosis. A. The number of apoptotic cells was detected by flow cytometry. B. Histogram summarizing the percentage of apoptotic cells (**, $P < 0.01$, compared to the NC group). C. The Bcl-2 protein level was determined using western blotting. D. Semi-quantitative analyses of the western blots (**, $P < 0.01$, compared to the NC group). Data were mean ± SD from three independent experiments.

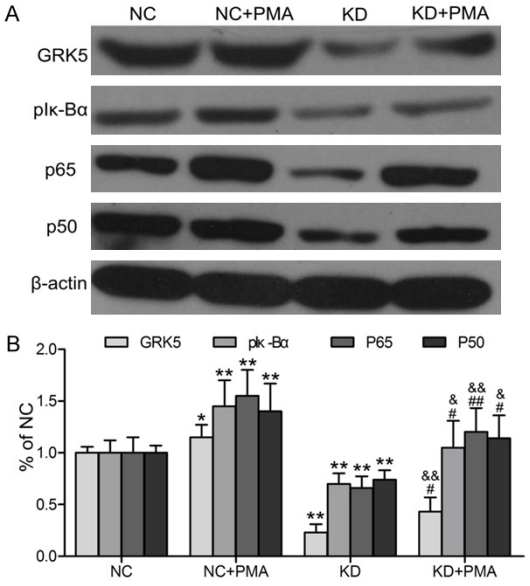

Figure 9. GRK5 knockdown affects NF-κB protein levels in glioblastoma cells. A. Representative western blots for GRK5, pIκBα, p65 and p50. GRK5 knockdown decreased the levels of pIκBα, p65 and p50 in glioblastoma cells, whereas treatment of cells with NF-κB stimulator PMA reversed this effect. The proteins levels of GRK5 and NF-κB increased in glioblastoma cells treated with PMA. B. Semi-quantitative analyses of the western blots. All protein bands were quantitatively analyzed as one band per lane. The units are arbitrary with control, and expressed as means ± SD. (*, $P < 0.05$; **, $P < 0.01$ versus the NC group. #, $P < 0.05$; ##, $P < 0.01$ versus the KD group. &, $P < 0.05$; &&, $P < 0.01$ versus the NC+PMA group. NC: NC group, KD: GRK5-KD group, pIκBα: phosphorylated IκBα). Data were mean ± SD from three independent experiments.

(independent-samples *t* test). Next, the depletion of GRK5 decreased the levels of pIκ-Bα, p65 and p50 in glioblastoma cells, and this effect was partially reversed after treatment with PMA (independent-samples *t* test). This study showed an interaction between GRK5 and NF-κB signaling in glioblastoma cells.

GRK5-NF-κB pathway affects the expressions of CCL2, IL6 and IL8 in the conditioned medium (CM) of glioblastoma cells

In addition, ELISA was used to quantify the levels of CCL2, IL-6 and IL-8 in the CM of glioblastoma cells (**Figure 10A-C**), which are the downstream cytokines and chemokines regulated by NF-κB signaling. Data analysis showed that all of the three secretory products decreased in the CM of glioblastoma cells after GRK5 knockdown. However, treatment of cells with PMA reversed this effect by increasing their levels (independent-samples *t* test).

Discussion

As one of the most studied GRKs, the role of GRK5 has been widely explored in various cancers. However, little is known in glioma biology regarding GRK5. High grade gliomas, especially GBM, exhibit a distinct cellular heterogeneity and differentiation hierarchy [52]. Glioma stem cells (GSCs), which are localized and maintained in the glioma niche, contribute to glioblastoma vascularization, cell proliferation and

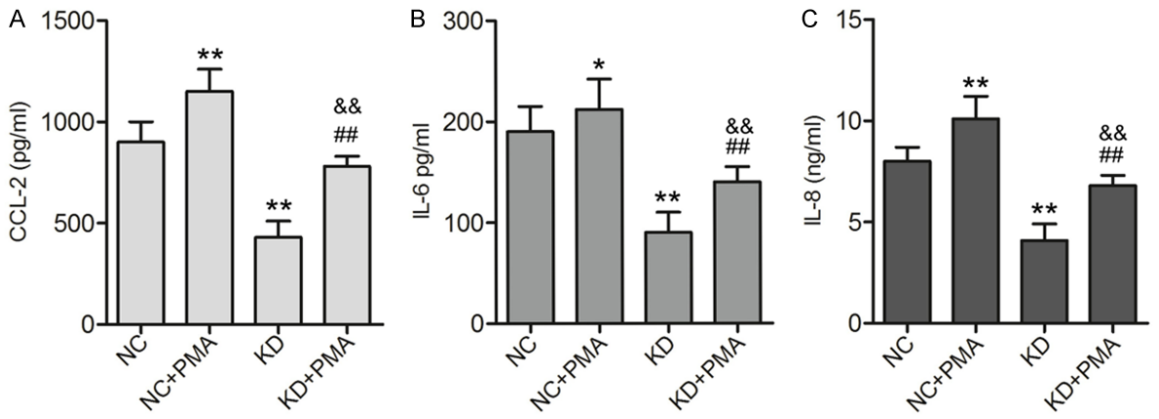

Figure 10. ELISA quantification of CCL2, IL6 and IL8 protein levels in the CM of glioblastoma cells. GRK5 knockdown decreased the levels of CCL2, IL-6 and IL-8 in the CM of glioma cells, whereas treatment of cells with PMA reversed this effect by increasing their levels (*, $P < 0.05$; **, $P < 0.01$ versus the NC group. #, $P < 0.05$; ##, $P < 0.01$ versus the KD group. &, $P < 0.05$; &&, $P < 0.01$ versus the NC+PMA group. NC: NC group, KD: GRK5-KD group). Data were mean ± SD from three independent experiments.

therapeutic resistance [52]. In this study, we observed that high expression of GRK5 was prevalent in gliomas and was positively correlated with pathological grade. It was noteworthy that GRK5 was proximal to the lumen of tumor blood vessels in human gliomas, especially in HGGs. This finding indicates that GRK5 expression may promote tumor angiogenesis in human gliomas. In addition, GRK5/CD133 co-expressing cells were detected in glioma specimens. Furthermore, most CD133+ cells co-expressed GRK5 in GBMs. These data suggest that GRK5 may be important for angiogenesis in gliomas as well as for maintaining of the tumorigenic potential of GSCs. Furthermore, GRK5 knockdown in the glioblastoma cell line U251 resulted in the attenuation of tumor cell proliferation, migration and invasion, and in the increase of apoptotic cells. The xenograft tumor model showed that GRK5-KD tumor xenografts grew slower than those of the NC and U251 groups. These results indicate that biological activity was altered in gliomas due to the loss of GRK5, and suggest that GRK5 is a potentially relevant target for therapy improvement. Thus, GRK5 deserves further investigation.

Members of the NF-κB family are important transcription factors that regulate cell invasion, cell proliferation, cell cycle progression and apoptosis in tumors [32-35]. Members of NF-κB family include RelB, cRel, p65 (RelA), p52, p50. Typically, the NF-κB pathway can be actived by phosphorylation of an IκB member. Members of the IκB family include NFκB1 (p105), NFκB2 (p100), IκBα, IκBβ and IκBε. Specifically, IκBα plays a crucial role in the initial activation of the NF-κB pathway [39]. Under unstimulated conditions, IκBα binds to p65 and p50. Upon stimulated conditions, IκBα undergoes rapid phosphorylation, followed by ubiquitination and degradation. As a result, p65 and p50 are released and, trafficked into the nucleus, where they evoke gene transcription [39]. Recent research has shown that GRK5 phosphorylates IκBα at Ser32/36, which are identical to those phosphorylated in IKKβ. Through the N-terminal domain of IκBα, GRK5 interacts with IκBα [39]. Furthermore, Islam [36] found that up-regulation of GRK5 increased the expression of p65 and p50 as well as promoted the DNA binding activity of the NF-κB pathway [36]. Conversely, other research has shown that NF-κB plays a critical role in the regulation of GRK5 transcription [50]. As a known stimulator of NF-κB, PMA not only increased the mRNA level of GRK5 and promoted the binding activity of NF-κB to the GRK5 promoter in vitro, but also enhanced recruitment of p65 and p50 to the GRK5 promoter region in vivo [50]. Both p65 and p50 can interact with the promoter of GRK5, as detected by ChIP and EMSA assays [50].

In this study, the effects of PMA treatment and GRK5 alteration on the NF-κB pathway in glioblastoma cells were detected by immunoblotting analysis. We down-regulated the GRK5 protein level in U251 cells in order to analyze changes in GRK5-NF-κB signaling. Firstly, we found increased p65, p50 and GRK5 expres-

sion at 24 h post-PMA treatment, suggesting that PMA successfully increased the expression of GRK5-NF-κB signaling in U251 cells. We next observed that the reduction in GRK5 was followed by a decrease in the protein levels of p65 and p50. Data analysis also showed an apparent phosphorylation of IκBα by PMA treatment, whereas the loss of GRK5 partly attenuated pIκBα. In short, our research demonstrated that GRK5 can interact with and affect the NF-κB pathway. The activation of GRK5-NF-κB signaling may be involved in glioma progression.

The tumor microenvironment is increasingly believed to have a key role in tumor development. Recent studies revealed that the NF-κB pathway can regulate the GBM secretory product [33]. The inhibition of the NF-κB pathway resulted in a decrease of various of cytokines and chemokines and their related pathways [33], in which IL6 prompted cell growth and invasion via autocrine mechanisms, IL8 contributed to angiogenesis, and CCL2 activated tumor-associated macrophages (TAMs) in a paracrine manner [33]. TAM infiltration promotes malignant progression of glioma by inducing extracellular matrix remodeling, angiogenesis and invasion [53]. TAMs are especially numerous in high-grade tumors [54-56]. Most TAMs surround glioma stem cells (GSCs), which play an important role in maintaining the plasticity and self-renewal of GSCs [57]. Inspiringly, as key downstream cytokines and chemokines of the NF-κB pathway, IL-6, IL-8 and CCL2 protein levels decreased in the CM of GBM cells after GRK5 knockdown, indicating that GRK5 indirectly adjusted GBM secreted products via the NF-κB pathway.

In summary, an alteration of GRK5 affects the biological activity of glioma cells, and the activation of the GRK5-NF-κB pathway is involved in the malignant progression of glioma. However, further studies are needed to explore GRK5-NF-κB signaling in glioma cells, GSCs and their tumor microenvironment.

Acknowledgements

The study was supported by National Natural Science Foundation of China (NO. 81172407), and the Science and Technology Project grant from Anhui Province (NO. 1606c08235, NO. 1604a0802069).

Disclosure of conflict of interest

None.

Address correspondence to: Chao-Shi Niu, Department of Neurosurgery, The First Affiliated Hospital of University of Science and Technology of China, Lujiang Road 17, Hefei 230001, Anhui Province, P. R. China. Tel: +8655162284149; E-mail: niuchaoshi@126.com

References

[1] Wang D, Zhi T, Xu X, Bao Z, Fan L, Li Z, Ji J, Liu N. MicroRNA-936 induces cell cycle arrest and inhibits glioma cell proliferation by targeting CKS1. Am J Cancer Res 2017; 7: 2131-2143.

[2] Rennert RC, Hoshide RR, Signorelli JW, Amaro D, Sack JA, Brennan CW, Chen CC. Concurrence of chromosome 6 chromothripsis and glioblastoma metastasis. J Neurosurg 2017; 126: 1472-1478.

[3] Nogués L, Palacios-García J, Reglero C, Rivas V, Neves M, Ribas C, Penela P, Mayor F Jr. G protein-coupled receptor kinases (GRKs) in tumorigenesis and cancer progression: GPCR regulators and signaling hubs. Semin Cancer Biol 2018; 48: 78-90.

[4] Oppermann M, Diversé-Pierluissi M, Drazner MH, Dyer SL, Freedman NJ, Peppel KC, Lefkowitz RJ. Monoclonal antibodies reveal receptor specificity among G-protein-coupled receptor kinases, Proc Natl Acad Sci U S A 1996; 93: 7649-7654.

[5] Willets JM, Challiss RA, Nahorski SR. Non-visual GRKs: are we seeing the whole picture? Trends Pharmacol Sci 2003; 24: 626-633.

[6] Gros R, Benovic JL, Tan CM, Feldman RD. G-protein-coupled receptor kinase activity is increased in hypertension. J Clin Invest 1997; 99: 2087-2093.

[7] Ungerer M, Böhm M, Elce JS, Erdmann E, Lohse MJ. Altered expression of beta-adrenergic receptor kinase and beta 1-adrenergic receptors in the failing human heart. Circulation 1993; 87: 454-463.

[8] Lombardi MS, Kavelaars A, Cobelens PM, Schmidt RE, Schedlowski M, Heijnen CJ. Adjuvant arthritis induces down-regulation of G protein-coupled receptor kinases in the immune system. J Immunol 2001; 166: 1635-1640.

[9] Suo Z, Cox AA, Bartelli N, Rasul I, Festoff BW, Premont RT, Arendash GW. GRK5 deficiency leads to early Alzheimer-like pathology and working memory impairment. Neurobiol Aging 2007; 28: 1873-1888.

[10] Wu JH, Zhang L, Fanaroff AC, Cai X, Sharma KC, Brian L, Exum ST, Shenoy SK, Peppel K,

Freedman NJ. G protein-coupled receptor kinase-5 attenuates atherosclerosis by regulating receptor tyrosine kinases and 7-transmembrane receptors. Arterioscler Thromb Vasc Biol 2012; 32: 308-316.
[11] Wu CC, Tsai FM, Shyu RY, Tsai YM, Wang CH, Jiang SY. G protein-coupled receptor kinase 5 mediates Tazarotene-induced gene 1-induced growth suppression of human colon cancer cells. BMC Cancer 2011; 11: 175.
[12] Tsai FM, Wu CC, Shyu RY, Wang CH, Jiang SY. Tazarotene-induced gene 1 inhibits prostaglandin E2-stimulated HCT116 colon cancer cell growth. J Biomed Sci 2011; 18: 88.
[13] Métayé T, Menet E, Guilhot J, Kraimps JL. Expression and activity of g protein-coupled receptor kinases in differentiated thyroid carcinoma. J Clin Endocrinol Metab 2002; 87: 3279-3286.
[14] Vassart G, Dumont JE. The thyrotropin receptor and the regulation of thyrocyte function and growth. Endocr Rev 1992; 13: 596-611.
[15] Paul MK, Mukhopadhyay AK. Tyrosine kinase-Role and significance in Cancer. Int J Med Sci 2004; 1: 101-115.
[16] Polakis P. Wnt signaling and cancer. Genes Dev 2000; 14:1837-1851.
[17] Wu JH, Goswami R, Cai X, Exum ST, Huang X, Zhang L, Brian L, Premont RT, Peppel K, Freedman NJ. Regulation of the platelet-derived growth factor receptor-beta by G protein-coupled receptor kinase-5 in vascular smooth muscle cells involves the phosphatase Shp2. J Biol Chem 2006; 281: 37758-37772.
[18] Chen M, Philipp M, Wang J, Premont RT, Garrison TR, Caron MG, Lefkowitz RJ, Chen W. G Protein-coupled receptor kinases phosphorylate LRP6 in the Wnt pathway. J Biol Chem 2009; 284: 35040-35048.
[19] Levine AJ. p53, the cellular gatekeeper for growth and division. Cell 1997; 88: 323-331.
[20] Bode AM, Dong Z. Post-translational modification of p53 in tumorigenesis. Nat Rev Cancer 2004; 4: 793-805.
[21] Toledo F, Wahl GM. Regulating the p53 pathway: in vitro hypotheses, in vivo veritas. Nat Rev Cancer 2006; 6: 909-923.
[22] Sorriento D, Del Giudice C, Bertamino A, Ciccarelli M, Gomez-Monterrey I, Campiglia P, Novellino E, Illario M, Trimarco B, De Luca N, Iaccarino G. New small molecules, ISA27 and SM13, inhibit tumour growth inducing mitochondrial effects of p53. Br J Cancer 2015; 112: 77-85.
[23] Chen X, Zhu H, Yuan M, Fu J, Zhou Y, Ma L. G-protein-coupled receptor kinase 5 phosphorylates p53 and inhibits DNA damage-induced apoptosis. J Biol Chem 2010; 285: 12823-12830.
[24] Arpin M, Chirivino D, Naba A, Zwaenepoel I. Emerging role for ERM proteins in cell adhesion and migration. Cell Adh Migr 2011; 5: 199-206.
[25] Mackay DJ, Esch F, Furthmayr H, Hall A. Rho- and rac-dependent assembly of focal adhesion complexes and actin filaments in permeabilized fibroblasts: an essential role for ezrin/radixin/moesin proteins. J Cell Biol 1997; 138: 927-938.
[26] Chakraborty PK, Zhang Y, Coomes AS, Kim WJ, Stupay R, Lynch LD, Atkinson T, Kim JI, Nie Z, Daaka Y. G protein-coupled receptor kinase GRK5 phosphorylates moesin and regulates metastasis in prostate cancer. Cancer Res 2014; 74: 3489-3500.
[27] So CH, Michal AM, Mashayekhi R, Benovic JL. G protein-coupled receptor kinase 5 phosphorylates nucleophosmin and regulates cell sensitivity to polo-like kinase 1 inhibition. J Biol Chem 2012; 287: 17088-17099.
[28] Iobagiu C, Lambert C, Raica M, Lima S, Khaddage A, Peoc'h M, Genin C. Loss of heterozygosity in tumor tissue in hormonal receptor genes is associated with poor prognostic criteria in breast cancer. Cancer Genet 2015; 208: 135-142.
[29] Thiagalingam S, Laken S, Willson JK, Markowitz SD, Kinzler KW, Vogelstein B, Lengauer C. Mechanisms underlying losses of heterozygosity in human colorectal cancers. Proc Natl Acad Sci U S A 2001; 98: 2698-2702.
[30] van Zelderen-Bhola S, Vink R, Smit J, Wessels H, Morreau H. Translocations (X;10)(p22;q24) and (1;10)(q21;q11) in a follicular adenoma of the thyroid without apparent involvement of the RET protooncogene. Cancer Genet Cytogenet 1999; 112: 178-180.
[31] Premont RT, Macrae AD, Aparicio SA, Kendall HE, Welch JE, Lefkowitz RJ. The GRK4 subfamily of G protein-coupled receptor kinases. Alternative splicing, gene organization, and sequence conservation. J Biol Chem 1999; 274: 29381-29389.
[32] Yang F, Liu X, Liu Y, Liu Y, Zhang C, Wang Z, Jiang T, Wang Y. miR-181d/MALT1 regulatory axis attenuates mesenchymal phenotype through NF-κB pathways in glioblastoma. Cancer Lett 2017; 396: 1-9.
[33] Zanotto-Filho A, Gonçalves RM, Klafke K, de Souza PO, Dillenburg FC, Carro L, Gelain DP, Moreira JC. Inflammatory landscape of human brain tumors reveals an NFκB dependent cytokine pathway associated with mesenchymal glioblastoma. Cancer Lett 2017; 390: 176-187.
[34] Kim SH, Ezhilarasan R, Phillips E, Gallego-Perez D, Sparks A, Taylor D, Ladner K, Furuta T, Sabit H, Chhipa R, Cho JH, Mohyeldin A, Beck S, Kurozumi K, Kuroiwa T, Iwata R, Asai A, Kim

J, Sulman EP, Cheng SY, Lee LJ, Nakada M, Guttridge D, DasGupta B, Goidts V, Bhat KP, Nakano I. Serine/Threonine kinase MLK4 determines mesenchymal identity in glioma stem cells in an NF-κB-dependent manner. Cancer Cell 2016; 29: 201-213.

[35] Li Y, Zhou QL, Sun W, Chandrasekharan P, Cheng HS, Ying Z, Lakshmanan M, Raju A, Tenen DG, Cheng SY, Chuang KH, Li J, Prabhakar S, Li M, Tergaonkar V. Non-canonical NF-κB signalling and ETS1/2 cooperatively drive C250T mutant TERT promoter activation. Nat Cell Biol 2015; 17: 1327-1338.

[36] Islam KN, Bae JW, Gao E, Koch WJ. Regulation of nuclear factor κB (NF-κB) in the nucleus of cardiomyocytes by G protein-coupled receptor kinase 5 (GRK5). J Biol Chem 2013; 288: 35683-35689.

[37] Parameswaran N, Pao CS, Leonhard KS, Kang DS, Kratz M, Ley SC, Benovic JL. Arrestin-2 and G protein-coupled receptor kinase 5 interact with NFkappaB1 p105 and negatively regulate lipopolysaccharide-stimulated ERK1/2 activation in macrophages. J Biol Chem 2006; 281: 34159-34170.

[38] Valanne S, Myllymäki H, Kallio J, Schmid MR, Kleino A, Murumägi A, Airaksinen L, Kotipelto T, Kaustio M, Ulvila J, Esfahani SS, Engström Y, Silvennoinen O, Hultmark D, Parikka M, Rämet M. Genome-wide RNA interference in drosophila cells identifies G protein-coupled receptor kinase 2 as a conserved regulator of NF-kappaB signaling. J Immunol 2010; 184: 6188-6198.

[39] Patial S, Luo J, Porter KJ, Benovic JL, Parameswaran N. G-protein-coupled-receptor kinases mediate TNFa-induced NFκB signalling via direct interaction with and phosphorylation of IκBα. Biochem J 2009; 425: 169-178.

[40] Patial S, Shahi S, Saini Y, Lee T, Packiriswamy N, Appledorn DM, Lapres JJ, Amalfitano A, Parameswaran N. G-protein coupled receptor kinase 5 mediates lipopolysaccharide-induced NFκB activation in primary macrophages and modulates inflammation in vivo in mice. J Cell Physiol 2011; 226: 1323-1333.

[41] Kleihues P, Louis DN, Scheithauer BW, Rorke LB, Reifenberger G, Burger PC, Cavenee WK. The WHO classification of tumors of the nervous system. J Neuropathol Exp Neurol 2002; 61: 215-225.

[42] Louis DN, Ohgaki H, Wiestler OD, Cavenee WK, Burger PC, Jouvet A, Scheithauer BW, Kleihues P. The 2007 WHO classification of tumours of the central nervous system. Acta Neuropathol 2007; 114: 97-109.

[43] Hao J, Song X, Song B, Liu Y, Wei L, Wang X, Yu J. Effects of lentivirus-mediated HIF-1alpha knockdown on hypoxia-related cisplatin resistance and their dependence on p53 status in fibrosarcoma cells. Cancer Gene Ther 2008; 15: 449-455.

[44] Niu CS, Yang Y, Cheng CD. MiR-134 regulates the proliferation and invasion of glioblastoma cells by reducing Nanog expression. Int J Oncol 2013; 42: 1533-1540.

[45] Livak KJ and Schmittgen TD. Analysis of relative gene expression data using real-time quantitative PCR and the 2(-Delta Delta C(T)) method. Methods 2001; 25: 402-408.

[46] Ye XZ, Xu SL, Xin YH, Yu SC, Ping YF, Chen L, Xiao HL, Wang B, Yi L, Wang QL, Jiang XF, Yang L, Zhang P, Qian C, Cui YH, Zhang X, Bian XW. Tumor-associated microglia/macrophages enhance the invasion of glioma stem-like cells via TGF-β1 signaling pathway. J Immunol 2012; 189: 444-453.

[47] Yang W, Xia Y, Ji H, Zheng Y, Liang J, Huang W, Gao X, Aldape K, Lu Z. Nuclear PKM2 regulates beta-catenin transactivation upon EGFR activation. Nature 2011; 480: 118-122.

[48] Yang Y, Niu CS, Cheng CD. Pin1-Nanog expression in human glioma is correlated with advanced tumor progression. Oncol Rep 2013; 30: 560-566.

[49] Mei X, Chen YS, Chen FR, Xi SY, Chen ZP. Glioblastoma stem cell differentiation into endothelial cells evidenced through live-cell imaging. Neuro Oncol 2017; 19: 1109-1118.

[50] Islam KN and Koch WJ. Involvement of nuclear factor κB (NF-κB) signaling pathway in regulation of cardiac G protein-coupled receptor kinase 5 (GRK5) expression. J Biol Chem 2012; 287: 12771-12778.

[51] Zhang Y, Shen GL, Shangguan LJ, Yu Y, He ML. Involvement of NFκB signaling in mediating the effects of GRK5 on neural stem cells. Brain Res 2015; 1608: 31-39.

[52] Zhou W, Ke SQ, Huang Z, Flavahan W, Fang X, Paul J, Wu L, Sloan AE, McLendon RE, Li X, Rich JN, Bao S. Periostin secreted by glioblastoma stem cells recruits M2 tumour-associated macrophages and promotes malignant growth. Nat Cell Biol 2015; 17: 170-182.

[53] Wesolowska A, Kwiatkowska A, Slomnicki L, Dembinski M, Master A, Sliwa M, Franciszkiewicz K, Chouaib S, Kaminska B. Microglia-derived TGF-beta as an important regulator of glioblastoma invasion--an inhibition of TGF-beta-dependent effects by shRNA against human TGF-beta type II receptor. Oncogene 2008; 27: 918-930.

[54] Hirota S, Miyamoto M, Kasugai T, Kitamura Y, Morimura Y. Crystalline light-chain deposition and amyloidosis in the thyroid gland and kidneys of a patient with myeloma. Arch Pathol Lab Med 1990; 114: 429-431.

[55] Roggendorf W, Strupp S and Paulus W. Distribution and characterization of microglia/macrophages in human brain tumors. Acta Neuropathol 1996; 92: 288-293.
[56] Morris CS and Esiri MM. Immunocytochemical study of macrophages and microglial cells and extracellular matrix components in human CNS disease. 1. Gliomas. J Neurol Sci 1991; 101: 47-58.
[57] Filatova A, Acker T and Garvalov BK. The cancer stem cell niche(s): the crosstalk between glioma stem cells and their microenvironment. Biochim Biophys Acta 2013; 1830: 2496-2508.

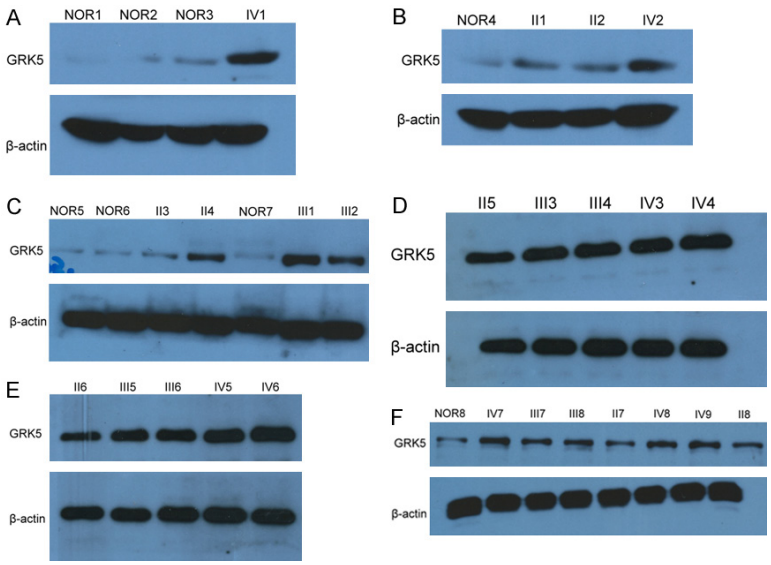

Figure S1. A-F. All of the original western images for total 33 samples (8 normal brain tissues, 8 WHO II samples, 8 WHO III samples and 9 WHO IV samples) in **Figure 1**.

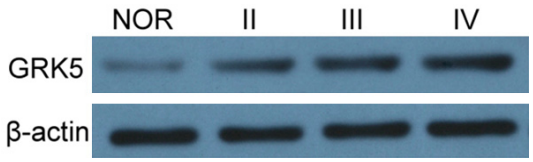

Figure S2. The original western images in **Figure 1A**.

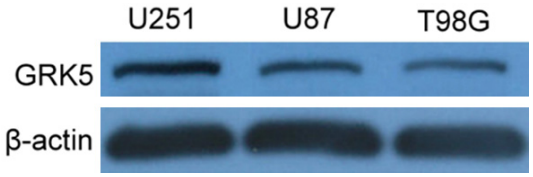

Figure S3. The original western images in **Figure 5A**.

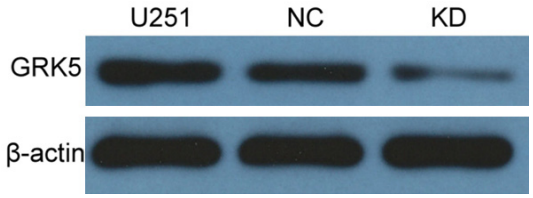

Figure S4. The original western images in **Figure 5D**.

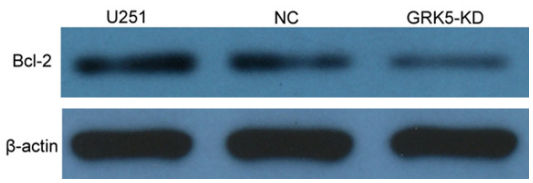

Figure S5. The original western images in **Figure 8C**.

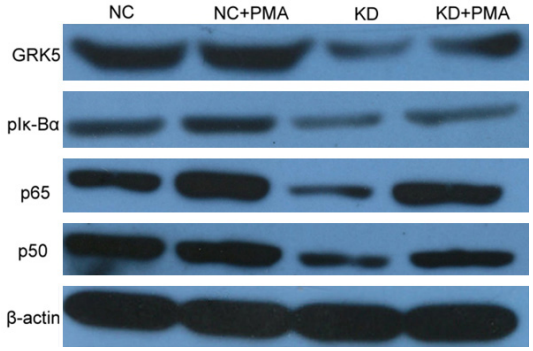

Figure S6. The original western images in **Figure 9A**.

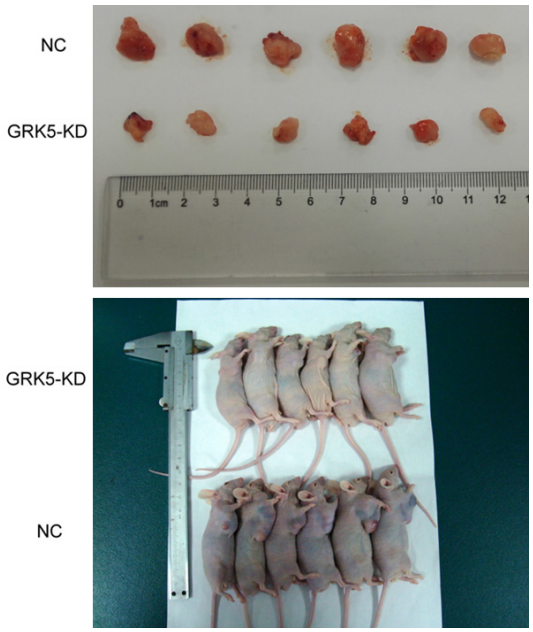

Figure S7. A human xenograft model was established.